Electron thermal conductivity owing to collisions between degenerate electrons

P. S. Shternin and D. G. Yakovlev

Ioffe Physical Technical Institute, Politekhnicheskaya 26, 194021 Saint-Petersburg, Russia

(Dated: 5th February 2008)

We calculate the thermal conductivity of electrons produced by electron-electron Coulomb scattering in a strongly degenerate electron gas taking into account the Landau damping of transverse plasmons. The Landau damping strongly reduces this conductivity in the domain of ultrarelativistic electrons at temperatures below the electron plasma temperature. In the inner crust of a neutron star at temperatures $T \lesssim 10^7$ K this thermal conductivity completely dominates over the electron conductivity due to electron-ion (electron-phonon) scattering and becomes competitive with the the electron conductivity due to scattering of electrons by impurity ions.

I. INTRODUCTION

The electron thermal conductivity is an important kinetic property of plasmas in experimental devices, in metals and semiconductors and in astrophysical objects. It has been studied for a long time and described in textbooks (see, e.g., Ziman [1], Lifshitz and Pitaevskiĭ [2]). We will show that some aspects of this problem have to be revised.

Specifically, we will consider the thermal conductivity of degenerate electrons. It is important in metals, semiconductors as well as in degenerate cores of evolved stars (giants, supergiants and, most importantly, white dwarfs), and in envelopes of neutron stars. It is needed to study cooling of white dwarfs (e.g., Prada Moroni and Straniero [3]) and nuclear explosions of massive white dwarfs as type Ia supernovae (e.g., Baraffe, Heger and Woosley [4]). In neutron star envelopes it is required for many reasons — for simulating cooling of isolated neutron stars (see, e.g., Lattimer et al. [5], Gnedin, Yakovlev and Potekhin [6], Page, Geppert and Weber [7]); for studying heat propagation and thermal relaxation in a neutron star envelope in response to the various processes of crustal energy release. In particular, these processes include pulsar glitches (e.g., Larson and Link [8], and references therein), deep crustal heating of accreting neutron stars in soft X-ray transients (e.g., Ushomirsky and Rutledge [9]), superbursts as powerful nuclear explosions at the base of the outer crust of an accreting neutron star (e.g., Strohmayer and Bildsten [10]; Page and Cumming [11]).

It is well known, that the electrons give the main contribution into the thermal conductivity of strongly degenerate matter. Their thermal conductivity can be written as

$$\kappa_e = \frac{\pi^2 T k_{\mathrm{B}}^2 n_e}{3 m_e^* \nu_e}, \quad \nu_e = \nu_{ei} + \nu_{ee}. \tag{1}$$

Here, T is the temperature, k_{B} is the Boltzmann constant, n_e is the number density of electrons, $m_e^* = \mu/c^2$, μ is the electron chemical potential (including the rest-mass term), and ν_e is the total effective electron collision frequency. The latter frequency is the sum of the partial collision frequencies ν_{ei} and ν_{ee}. In ν_{ei} we include all collisions of electrons mediated by their interactions with ions (direct Coulomb scattering of electrons by ions in an ion gas or liquid; electron-phonon scattering in an ion crystal and electron scattering by impurity ions at low temperatures). Evidently, Eq. (1) can be rewritten as

$$\frac{1}{\kappa_e} = \frac{1}{\kappa_{ei}} + \frac{1}{\kappa_{ee}}, \quad \kappa_{ei} = \frac{\pi^2 T k_{\mathrm{B}}^2 n_e}{3 m_e^* \nu_{ei}},$$
$$\kappa_{ee} = \frac{\pi^2 T k_{\mathrm{B}}^2 n_e}{3 m_e^* \nu_{ee}}, \tag{2}$$

where the partial conductivities κ_{ei} and κ_{ee} are determined, respectively, by the ei and ee collisions.

It is widely believed that the dominant contribution into κ_e comes from the ei collisions. The associated partial conductivity κ_{ei} has been studied in a number of papers (e.g., Potekhin et al. [12], Gnedin et al. [6] and references therein). The partial thermal conductivity κ_{ee} owing to the ee collisions was calculated by Lampe [13], Flowers and Itoh [14], Urpin and Yakovlev [15], and Timmes [16]. These calculations were summarized by Potekhin et al. [12]. The main result was that the ee collisions are mainly negligible, except for a hot low-density plasma of light elements (from hydrogen to carbon) with the temperature a few times lower than the electron degeneracy temperature (in that case the ee collisions did affect κ_e but never dominated as long as the electrons were degenerate; see Lampe [13]; Urpin and Yakovlev [15]).

However, all these calculations have neglected an important effect of the Landau damping of the ee interaction owing to the exchange of transverse plasmons. In the context of transport properties of dense matter this effect was studied by Heiselberg and Pethick [17] for degenerate quark plasmas. Similar effects have recently been analyzed by Jaikumar, Gale and Page [18] for neutrino bremsstrahlung radiation in the ee collisions. Here we reconsider κ_{ee} including the effects of the Landau damping and show that κ_{ee} is actually much more important than thought before.

II. FORMALISM

We analyze the thermal conductivity κ_{ee} of strongly degenerate electrons under the conditions that the electrons constitute an almost ideal and uniform Fermi gas and collide between themselves and with plasma ions. Although the results will be more important for ultrarelativistic electrons, our consideration will be general and valid for both, relativistic and non-relativistic, cases. We will use the same standard variational approach with the simplest trial non-equilibrium electron distribution function as Flowers and Itoh [14]. The calculations are similar to those performed by Heiselberg and Pethick [17] for the thermal conductivity of quarks; thus we omit the details.

Following Heiselberg and Pethick [17] we have

$$
\begin{aligned}
\nu_{ee} = & \frac{3\hbar^3}{8 v_e p_e^2 (k_B T)^3} \int \frac{d\boldsymbol{p}_1\, d\boldsymbol{p}_2\, d\boldsymbol{p}_1'\, d\boldsymbol{p}_2'}{(2\pi\hbar)^{12}} \\
& \times W(12|1'2')\, f_1 f_2 (1 - f_1')(1 - f_2') \\
& \times [\boldsymbol{v}_1\,(\varepsilon_1 - \mu) + \boldsymbol{v}_2\,(\varepsilon_2 - \mu) - \boldsymbol{v}_1'\,(\varepsilon_1' - \mu) \\
& - \boldsymbol{v}_2'\,(\varepsilon_2' - \mu)]^2,
\end{aligned}
\tag{3}
$$

where $p_e = \hbar (3\pi^2 n_e)^{1/3}$ and $v_e = p_e/m_e^*$ are, respectively, the electron Fermi momentum and Fermi velocity; the integration is over all allowable ee collisions $\boldsymbol{p}_1 \boldsymbol{p}_2 \to \boldsymbol{p}_1' \boldsymbol{p}_2'$; $\boldsymbol{p}$ is an electron momentum, $\boldsymbol{v}$ its velocity, ε its energy; primes refer to electrons after a collision event; f is the electron Fermi-Dirac distribution, and $W(12|1'2')$ is the differential transition probability

$$
\begin{aligned}
W(12|1'2') = & 4\,(2\pi\hbar)^6\, \delta(\varepsilon_1' + \varepsilon_2' - \varepsilon_1 - \varepsilon_2) \\
& \times \delta(\boldsymbol{p}_1' + \boldsymbol{p}_2' - \boldsymbol{p}_1 - \boldsymbol{p}_2)\, |M_{fi}|^2, \quad (4)
\end{aligned}
$$

$|M_{fi}|^2$ being the squared matrix element summed over electron spin states. The symmetry factors required to avoid double counting of the same initial and final electron states are also included into $|M_{fi}|^2$.

The multi-dimensional integral (3) is simplified further using the standard angular-energy decomposition (separating integrations over particle energies and orientations of their momenta; e.g., Shapiro and Teukolsky [19]). Because the electrons are strongly degenerate, they can participate in thermal conduction only if their energies are close to the Fermi level. Accordingly, their momenta can be placed at the Fermi surface in angular integrals whenever possible. Characteristic energy transfers $\hbar\omega \equiv \varepsilon_1' - \varepsilon_1$ in collisions of strongly degenerate particles are small, $\hbar\omega \lesssim k_B T$. Momentum transfers $\hbar\boldsymbol{q} \equiv \boldsymbol{p}_1' - \boldsymbol{p}_1$ are also small, $\hbar q \ll p_e$, owing to a long-range nature of the Coulomb interaction. We will use this small-momentum-transfer approximation throughout the paper. Typical values of $\hbar q$ are determined by plasma screening of the Coulomb interaction.

The plasma screening was thoroughly analyzed by Heiselberg and Pethick [17]. These authors studied quark-quark interaction through one-gluon exchange in the weak-coupling limit which is very similar to the Coulomb interaction in an ordinary plasma. The matrix element for an ee scattering event is $M_{fi} = M_{fi}^{(1)} + M_{fi}^{(2)}$, where $M_{fi}^{(1)}$ and $M_{fi}^{(2)}$ correspond to the channels $1 \to 1'; 2 \to 2'$ and $1 \to 2'; 2 \to 1'$, respectively. For instance,

$$
M_{fi}^{(1)} \propto \frac{J_{1'1}^{(0)} J_{2'2}^{(0)}}{q^2 + \Pi_l} - \frac{\boldsymbol{J}_{t1'1} \cdot \boldsymbol{J}_{t2'2}}{q^2 - \omega^2/c^2 + \Pi_t},
\tag{5}
$$

where $J_{e'e}^{(\nu)} = (J_{e'e}^{(0)}, \boldsymbol{J}_{e'e}) = c\,(\bar{u}_{e'} \gamma^\nu u_e)$ is the transition 4-current ($\nu = 0, 1, 2, 3$), $\boldsymbol{J}_{te'e}$ is the component of $\boldsymbol{J}_{e'e}$ transverse to $\boldsymbol{q}$, γ^ν is a Dirac matrix, u_e is a normalized electron bispinor ($\bar{u}_e u_e = 2 m_e c^2$), and $\bar{u}_e$ is a Dirac conjugate (see, e.g., Berestetskiĭ, Lifshitz and Pitaevskii [20]). The longitudinal component of $\boldsymbol{J}_{e'e}$ (parallel to $\boldsymbol{q}$) is related to the time-like (charge density) component $J_{e'e}^{(0)}$ via current continuity equation; it is excluded from Eq. (5), see Ref. [17].

The polarization functions Π_l and Π_t in Eq. (5) depend on ω and q and describe the plasma screening of the ee interaction through the exchange of longitudinal and transverse plasmons, respectively. In the classical limit ($\hbar q \ll p_e$ and $\hbar \omega \ll v_e p_e$), taking into account the polarization produced by degenerate electrons in the first-order random phase approximation, one has (e.g., Alexandrov, Bogdankevich and Rukhadze [21])

$$
\Pi_l = q_0^2 \chi_l(x), \qquad \Pi_t = (q_0 v_e/c)^2 \chi_t(x),
\tag{6}
$$

where $x = \omega/(q v_e)$,

$$
\begin{aligned}
\chi_l(x) &= 1 - \frac{x}{2}\,\ln\left(\frac{x+1}{x-1}\right), \\
\chi_t(x) &= \frac{x^2}{2} + \frac{x(1-x^2)}{4}\,\ln\left(\frac{x+1}{x-1}\right),
\end{aligned}
\tag{7}
$$

with

$$
\hbar^2 q_0^2 = 4 e^2 p_e^2 / (\pi \hbar v_e),
\tag{8}
$$

q_0 being the ordinary Thomas-Fermi electron screening wavenumber. Particularly, in the limit of $\omega \to 0$ and $\omega/q \ll v_e$ we have

$$
\chi_l = 1, \qquad \chi_t = i\,\pi\omega/(4 q v_e).
\tag{9}
$$

According to Eqs. (5) and (6), the plasma screening of the ee current interaction via the exchange of transverse plasmons (the second term in Eq. (5)) is different from the screening of the charge interaction via the exchange of longitudinal plasmons (the first term). The difference results from the difference of the polarization functions Π_t and Π_l and has been neglected in all previous calculations of the electron thermal conductivity (where one has commonly set $\Pi_t = \Pi_l = q_0^2$, and $q^2 - (\omega/c)^2 + \Pi_t = q^2 + q_0^2$). Naturally, this difference is expected to be small for non-relativistic electrons ($v_e \ll c$), where the transverse current interaction term is small in the matrix element. We will see that the difference becomes important for relativistic electrons ($v_e \approx c$).

Let us recall that the functions Π_l and Π_t have real parts which describe plasmon refraction, and imaginary parts which describe plasmon absorption. In the ee scattering we deal with low-energy virtual plasmons, $\hbar\omega \lesssim k_B T$. As seen from Eq. (9), longitudinal plasmons undergo refraction which results in the Debye-type (Thomas-Fermi) screening of the Coulomb interaction, with the screening momentum (inverse screening length) q_0. As for transverse plasmons, they mainly undergo collisionless absorption (that is the Landau damping) by degenerate electrons. Their effect is drastically different from the effect of longitudinal plasmons.

The calculations similar to those in Ref. [17] lead to the following expressions for the ee collision frequency and thermal conductivity,

$$\nu_{ee} = \frac{36 n_e \alpha^2 \hbar^2 c I(u,\theta)}{\pi m_e^* k_B T}, \qquad \kappa_{ee} = \frac{\pi^3 k_B^3 T^2}{108 \alpha^2 \hbar^2 c I(u,\theta)}. \tag{10}$$

Here, $\alpha = e^2/\hbar c$ is the fine structure constant, and

$$
\begin{aligned}
I(u,\theta) =\ & \frac{1}{u} \int_0^\infty dw\, \frac{w\, e^w}{(e^w - 1)^2} \int_0^1 dx\, x^2 (1 - x^2) \\
& \times \int_0^\pi \frac{d\phi}{\pi} (1 - \cos\phi) \left| \frac{1}{1 + (x\theta/w)^2 \chi_l(x)} \right. \\
& \left. - \frac{u^2(1-x^2)\cos\phi}{1 - u^2 x^2 + u^2 (x\theta/w)^2 \chi_t(x)} \right|^2
\end{aligned} \tag{11}
$$

is a dimensionless function of two variables,

$$u \equiv v_e/c, \qquad \theta = \hbar v_e q_0/(k_B T) = \sqrt{3} T_{pe}/T, \tag{12}$$

$T_{pe} = \hbar\omega_{pe}/k_B$ being the electron plasma temperature determined by the electron plasma frequency $\omega_{pe} = \sqrt{4\pi e^2 n_e/m_e^*}$. Both components of the matrix element, $M_{fi}^{(1)}$ and $M_{fi}^{(2)}$, give equal contributions into Eq. (11), and the interference term is negligibly small because of the small-momentum-transfer approximation. Furthermore, $w = \hbar\omega/k_B T$; ϕ is the angle between $\boldsymbol{p}_{1t}$ and $\boldsymbol{p}_{2t}$, the components of $\boldsymbol{p}_1$ and $\boldsymbol{p}_2$ transverse to $\boldsymbol{q}$; and the integration over ϕ is trivial. Equations (10) and (11) are natural generalizations of Eqs. (58) and (59) of Heiselberg and Pethick [17] to the case of a degenerate gas of particles of arbitrary degree of relativity (in our case v/c may be arbitrary while in Ref. [17] $v = c$). The difference of numerical factors in the expressions for κ in our Eq. (10) and in Eq. (58) of Ref. [17] (108 versus 24) stems from the difference of physical systems under consideration (an electron gas versus a gas of light quarks interacting through gluon exchange).

III. FOUR REGIMES OF ELECTRON-ELECTRON COLLISIONS

Thus the collision frequency and the thermal conductivity (10) are solely determined by the electron number density and the temperature. Their calculation reduces to the calculation of the function $I(u,\theta)$ from Eq. (11). Clearly, the function can be written as

$$I = I_l + I_t + I_{lt}, \tag{13}$$

where I_l is the contribution from the ee interaction via the exchange of longitudinal plasmons (the first term in the squared modulus); I_t comes from the interaction via the exchange of transverse plasmons (the second term); and I_{lt} is the mixed term.

The analysis reveals four regimes (I–IV) of ee collisions in a strongly degenerate electron gas. These regimes are summarized in Table I. The regimes I and II are realized for non-relativistic electrons, while in the regimes III and IV electrons are ultrarelativistic. The regimes I and III take place for sufficiently high temperatures $T \gtrsim T_{pe}$, at which the Pauli principle does not restrict energy transfers between colliding electrons ($\hbar\omega < k_B T$; see, e.g., Lampe [13], especially his Fig. 1). The regimes II and IV refer to a colder electron gas, where energy transfers are essentially limited by the Pauli blocking (e.g., Lampe [13] and Flowers and Itoh [14]).

The analysis of Eq. (11) gives the following asymptotic values of I in the different regimes.

In the regime I (where $u \lesssim 1$ and $\theta \lesssim 1$)

$$
\begin{aligned}
I_l &= \frac{1}{u} \left(\frac{2}{15} \ln \frac{1}{\theta} + 0.1657 \right), \\
I_t &= u^3 \left(\frac{8}{315} \ln \frac{1}{\theta u} + 0.05067 \right), \\
I_{lt} &= u \left(\frac{8}{105} \ln \frac{1}{\theta} + 0.1236 \right).
\end{aligned} \tag{14}
$$

The logarithmic terms in brackets represent Coulomb logarithms, while the second terms are the corrections calculated using the standard technique [13]. The leading contribution comes from I_l. It was calculated by Lampe [13], with a slightly less accurate correction term ($1.30 \times 2/15 \approx 0.173$ from his Eqs. (5.22) and (5.23), instead of our 0.1657). Retaining this term in the regime I, one has $I = I_l$ and

$$\kappa_{ee} = \frac{5\pi^3 k_B^3 T^2 v_e}{72 \alpha^2 \hbar^2 c^2 [\ln(1/\theta) + 1.242]}. \tag{15}$$

Table I: Four regimes of thermal conduction of degenerate electrons owing to ee collisions.

Regime	Electron velocity	Temperature	Main contribution	T-dependence of κ_{ee}
I	$v_e \ll c$	$T \gtrsim T_{pe}$	I_l	$T^2/\ln(T/T_{pe})$
II	$v_e \ll c$	$T \ll T_{pe}$	I_l	$1/T$
III	$v_e \approx c$	$T \gtrsim T_{pe}$	$I_l + I_t + I_{lt}$	$T^2/\ln(T/T_{pe})$
IV	$v_e \approx c$	$T \ll T_{pe}$	I_t	const

Note that for I_t the regime I extends to lower temperatures $T \sim uT_{pe}$, than for I_l and I_{lt}, but this circumstance does not affect noticeably the thermal conductivity κ_{ee} because I_t is relatively insignificant in the given regime.

In the regime III (where $u \approx 1$ and $\theta \lesssim 1$),

$$
\begin{aligned}
I_l &= 2I_t = \frac{2}{15} \ln \frac{1}{\theta} + 0.1657, \\
I_{lt} &= \frac{2}{15} \ln \frac{1}{\theta} + 0.1399, \\
I &= \frac{1}{3} \ln \frac{1}{\theta} + 0.3884.
\end{aligned} \tag{16}
$$

Again, the logarithmic terms are Coulomb logarithms and the second terms are corrections. In this case, all terms (I_l, I_t, and I_{lt}) give comparable contributions into I. The asymptote of I in this regime was obtained by Heiselberg and Pethick [17] (their Eq. (60), with a slightly less accurate correction factor 0.30 instead of our 0.3884) in their studies of quark plasma. For an electron plasma, the conductivity κ_{ee} in the regime III was calculated by Urpin and Yakovlev [15]. Their result is equivalent to Eq. (16) for I but with less accurate correction ($\ln(2)/3 \approx 0.231$ instead of 0.3884) because they erroneously used the approximation of static longitudinal electron screening of the Coulomb interaction in all terms (with $\Pi_l = \Pi_t = q_0^2$ in Eq. (6)). Employing I from Eq. (16) in the regime III we obtain

$$
\kappa_{ee} = \frac{\pi^3 k_B^3 T^2}{36 \alpha^2 \hbar^2 c \left[\ln(1/\theta) + 1.165\right]}. \tag{17}
$$

In the regimes II and IV (where $\theta \gtrsim 1$ and $u \leq 1$ is arbitrary) we have

$$
I_l = \frac{\pi^5}{15 u \theta^3}, \quad I_t = 2\zeta(3) \frac{u}{\theta^2}, \quad I_{lt} = \frac{\xi}{\theta^{8/3}} u^{1/3}, \tag{18}
$$

$$
\xi = \frac{(2\pi)^{2/3}}{3} \Gamma\left(\frac{14}{3}\right) \zeta\left(\frac{11}{3}\right) \approx 18.52,
$$

where $\zeta(z)$ is the Riemann zeta function (with $\zeta(3) = 1.202$) and $\Gamma(z)$ is the gamma function. The expression for I_t (with $u = 1$) was obtained by Heiselberg and Pethick [17] for an ultrarelativistic quark plasma.

The asymptotic expressions (18) are derived from Eq. (11) with the screening functions χ_l and χ_t given by Eq. (9). In this approximation the screening of the ee interaction via the exchange of longitudinal plasmons (the first part of the matrix element in Eq. (5)) is described by $q^2 + \Pi_l \approx q^2 + q_0^2$, which is equivalent to the static Debye-type screening with the screening wavenumber $q_{\text{scr},l} = q_0$. The screening via the exchange of transverse plasmons (the second part of the matrix element) is more complicated. It is described by the denominator term $q^2 - \omega^2/c^2 + \Pi_t \approx q^2 + iq_0^2 \pi \omega v_e/(4qc^2)$ that represents the dynamical screening via the Landau damping of transverse plasmons, with $\hbar\omega \sim k_B T \ll v_e \hbar q$ (i.e., with low phase velocities $\omega/q \ll v_e$). In this case the effective screening wavenumber $q_{\text{scr},t}$ is evidently given by $q_{\text{scr},t}^3 \sim q_0^2 \omega v_e/c^2 \sim q_0^2 k_B T v_e/(\hbar c^2)$.

Using Eqs. (10) and (13) we can decompose the collision frequency ν_{ee} into the same parts as I, $\nu_{ee} = \nu_{ee}^{(l)} + \nu_{ee}^{(t)} + \nu_{ee}^{(lt)}$. One can easily see, that in the regimes II and IV the partial frequency $\nu_{ee}^{(l)}$ can be estimated as $\nu_{ee}^{(l)} \sim n_e \alpha^2 (k_B T)^2/(\hbar q_{\text{scr},l}^3 \mu)$. The collision frequency $\nu_{ee}^{(t)}$ can be estimated as $\nu_{ee}^{(t)} \sim u^4 \nu_{ee}^{(l)}$ by replacing $q_{\text{scr},l} \to q_{\text{scr},t}$. The factor u^4 takes into account the reduction of the ee interaction via transverse plasmons in the nonrelativistic electron gas. The quantity $\nu_{ee}^{(lt)}$ can be estimated as $\nu_{ee}^{(lt)} \sim u^2 \nu_{ee}^{(l)}$ with $q_{\text{scr},l}^3 \to q_{\text{scr},l}^2 q_{\text{scr},t}$.

In the regime II, where $\theta \gtrsim 1$ and $u \ll 1$, the exchange of longitudinal plasmons dominates, and we have $I \approx I_l$,

$$
\kappa_{ee} = \frac{5\hbar q_0^3 v_e^4}{36\pi^2 T \alpha^2 c^2}. \tag{19}
$$

This leading part of κ_{ee} in the regime II was calculated by Lampe [13]. Note that the asymptotic expression (18) for I_t at $u \ll 1$ is actually valid not at $T \lesssim T_{pe}$, as the expressions for I_l and I_{lt}, but at lower $T \lesssim uT_{pe}$. However, this circumstance is relatively unimportant because it is I_l which dominates in the regime II.

In the regime IV, where $\theta \gtrsim 1$ and $u \approx 1$, the exchange of transverse plasmons dominates, with $I \approx I_t$, and

$$
\kappa_{ee} = \frac{\pi^3 k_B c q_0^2}{216 \zeta(3) \alpha^2}. \tag{20}
$$

It is remarkable that in this regime κ_{ee} becomes temperature independent. This regime has been discussed in detail by Heiselberg and Pethick [17] for quark plasma. For the electron plasma, it was considered by Flowers and Itoh [14] and also by Urpin and Yakovlev [15] but both groups erroneously used the approximation of static longitudinal screening in all channels ($\chi_l = \chi_t = 1$) which strongly underestimates the efficiency of the plasma screening of the ee interaction in the ultrarelativistic electron gas. If that approximation were true, one would obtain $\nu_{ee}^{(l)} = \nu_{ee}^{(lt)} = 2\nu_{ee}^{(t)}$ and $\nu_{ee} = 2.5\nu_{ee}^{(l)}$, whereas in fact $\nu_{ee}^{(l)} \ll \nu_{ee}^{(lt)} \ll \nu_{ee}^{(t)}$ in the regime IV, and κ_{ee} is significantly lower than predicted by the previous calculations [14, 15].

Let us note that the temperature behavior of κ_{ee} (Table I) corresponds to an ordinary Fermi-liquid (where $\kappa \propto 1/T$; e.g., Baym and Pethick [22]) only in the regime II. In the regimes I and III the plasma is too warm (although degenerate) to reach the Fermi-liquid limit, where energy transfers between colliding particles are strongly restricted by the Pauli principle. In the regime IV the plasma is cold but the matrix element of the ee interaction essentially depends on energy transfers $\hbar\omega$ owing to the Landau damping of transverse plasmons which violates the Fermi-liquid behavior [17].

To facilitate applications, we have calculated the functions I_l, I_t and I_{lt} from Eq. (11) for a dense grid of u and θ and fitted the numerical data by analytic functions. We

obtain

$$I_l = \frac{1}{u} \left(0.1587 - \frac{0.02538}{1 + 0.0435\,\theta} \right)$$
$$\times \ln \left(1 + \frac{128.56}{37.1\,\theta + 10.83\,\theta^2 + \theta^3} \right). \quad (21)$$

Therefore, I_l is inversely proportional to u, with the proportionality coefficient dependent solely on θ. Furthermore,

$$I_t = u^3 \left(\frac{2.404}{C} + \frac{C_2 - 2.404/C}{1 + 0.1\,\theta\,u} \right)$$
$$\times \ln \left(1 + \frac{C}{A\,\theta\,u + \theta^2\,u^2} \right), \quad (22)$$

where $A = 20 + 450\,u^3$, $C = A\exp(C_1/C_2)$, $C_1 = 0.05067 + 0.03216\,u^2$, and $C_2 = 0.0254 + 0.04127\,u^4$. Finally,

$$I_{lt} = u \left(\frac{18.52\,u^2}{C} + \frac{C_2 - 18.52\,u^2/C}{1 + 0.1558\,\theta^B} \right)$$
$$\times \ln \left(1 + \frac{C}{A\theta + 10.83\,\theta^2 u^2 + (\theta u)^{8/3}} \right), \quad (23)$$

where $A = 12.2 + 25.2\,u^3$, $B = 1 - 0.75\,u$, $C = A\exp(C_1/C_2)$, $C_1 = 0.123636 + 0.016234\,u^2$, and $C_2 = 0.0762 + 0.05714\,u^4$. These fit expressions reproduce also all asymptotic limits mentioned above. The maximum fit errors of I_l, I_t, and I_{lt} are, respectively, 0.2% (at $u = 0.61$ and $\theta = 3.8$), 6.3% (at $u = 0.878$ and $\theta \sim 0.175$, where the electrons become nondegenerate) and 8.4% (at $u = 0.19$ and $\theta = 19$). The maximum fit error of the total function I in Eq. (13) is 2.5% (at $u = 0.924$ and $\theta = 0.232$).

IV. DISCUSSION

Let us discuss the efficiency of ee collisions for thermal conduction in a degenerate electron gas. Figure 1 shows the temperature-density diagram for a dense matter. For certainty, we have adopted the model of cold-catalyzed (ground-state) matter. It is composed of electrons and ions (atomic nuclei) at densities smaller than the neutron drip density $\rho_{\rm nd} \approx 4\times10^{11}$ g cm^{-3} (the right vertical dotted line), with an addition of free neutrons at higher densities ρ. The composition of the cold-catalyzed matter is taken from Haensel and Pichon [23] at $\rho < \rho_{\rm nd}$ and from Negele and Vautherin [24] at higher ρ. Weak first-oder phase transitions which accompany changes of ground-state nuclides with the growth of ρ are smoothed out as described by Kaminker et al. [25]. At $\rho \lesssim 10^8$ g cm^{-3} the ground-state matter is composed of iron (^{56}Fe). The densities $\rho \lesssim 10^9$ g cm^{-3} are appropriate for degenerate stellar cores of white dwarfs and evolved stars; the densities $\rho \lesssim 10^{14}$ are appropriate for envelopes (crusts) of neutron stars.
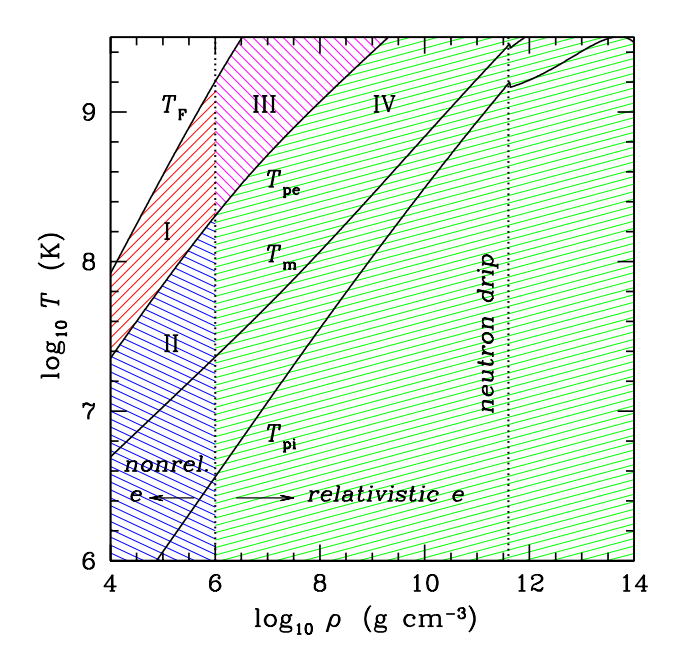

Figure 1: (color online) Temperature-density diagram for cold-catalyzed matter. We show the electron degeneracy temperature $T_{\rm F}$, the electron plasma temperature T_{pe}, the melting temperature $T_{\rm m}$ of the ion crystal, and the ion plasma temperature T_{pi}. The left dotted line separates the regions of a low-density non-relativistic electron gas and a denser gas of ultrarelativistic electrons. The right dotted line indicates the neutron drip point. Shaded regions I–IV show the $T - \rho$ domains of the different ee collision regimes (Table I).

In Figure 1 we plot the electron degeneracy temperature $T_{\rm F} = (\mu - m_e c^2)/k_{\rm B}$, the electron plasma temperature T_{pe}, the melting temperature of the ion crystal $T_{\rm m} \approx Z_i^2 e^2/(175 a k_{\rm B})$, and the ion plasma temperature $T_{pi} = \hbar\omega_{pi}/k_{\rm B}$ (where $\omega_{pi} = \sqrt{4\pi Z_i^2 e^2 n_i/m_i}$ is the ion plasma frequency, $Z_i e$ is the ion charge, m_i is its mass, n_i is the ion number density, and $a = (4\pi n_i/3)^{-1/3}$ is the ion-sphere radius). The left vertical dotted line separates the regions of non-relativistic degenerate electrons ($v_e \ll c$, $\rho \ll 10^6$ g cm^{-3}) and ultrarelativistic electrons ($v_e \to c$, $\rho \gg 10^6$ g cm^{-3}). The shaded regions I–IV show the temperature-density domains with the different regimes of ee collisions in a degenerate electron gas (see Section III, Table I).

In order to explore the importance of the ee collisions for thermal conduction let us compare κ_{ee} with the thermal conductivity κ_{ei} owing to ei collisions (Section I). The conductivity κ_{ei} is calculated using the formalism of Potekhin et al. [12] and Gnedin et al. [6].

In Figure 2 we plot the temperature dependence of the electron thermal conductivity of helium (^{4}He) or carbon (^{12}C) plasmas at $\rho = 10^5$ g cm^{-3} (left) or 10^6 g cm^{-3} (right). At $\rho = 10^5$ g cm^{-3} the electrons are nonrelativistic while at $\rho = 10^6$ g cm^{-3} they are mildly relativistic. According to Eq. (2), the total electron thermal conductivity κ_e is determined by the partial contributions κ_{ee}
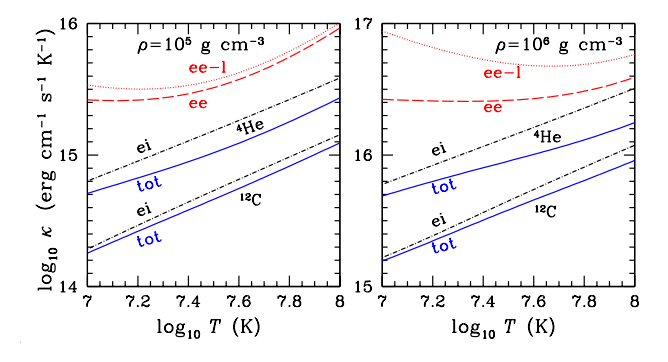
Figure 2: (color online) Temperature dependence of the electron thermal conductivity at $\rho = 10^5$ g cm^{-3} (*left*) and 10^6 g cm^{-3} (*right*). The dashed line *ee* shows κ_{ee}; the dotted line $ee-l$ is the same but retaining the contribution of longitudinal plasmons alone. The dot-and-dashed lines show κ_{ei} and the solid lines show the total (tot, $ee+ei$) conductivity κ_e for helium and carbon plasmas.

Figure 3: (color online) Density dependence of the electron thermal conductivity at different T (marked by the values of $\log_{10} T$ near the curves) in a neutron star crust composed of ground-state matter; the vertical dotted line is the neutron drip point. Dot-and-dashed lines (*ei*) show the conductivity κ_{ei} owing to *ei* collisions at $T = 10^7$, 10^8, and 10^9 K in a crystal of atomic nuclei for pure ground-state matter. In addition, the lower dot-and-dashed line at $T = 10^7$ K shows κ_{ei} which includes the contribution of electron scattering by impurity nuclei at $T = 10^7$ K (for $n_{\rm imp}/n_i = 0.05$ and $|Z_{\rm imp} - Z_i| = 2$). The dashed line is κ_{ee}; it is almost independent of T. The dotted line is the partial conductivity $\kappa_{ee}^{(l)}$ mediated by longitudinal plasmons alone at $T = 10^8$ K; it scales as T^{-1}. The solid lines show the total electron conductivity κ_e at $T = 10^7$ K for the matter without and with impurities. If $T \gtrsim 10^8$ K the effect of impurities is weak and $\kappa_e \approx \kappa_{ei}$.

and κ_{ei}, a minimum partial contribution being most important. The total conductivities are shown by the solid lines; κ_{ei} by the dot-and-dashed lines; κ_{ee} is plotted by the dashed lines (the same for the helium and carbon plasmas); the dotted lines give κ_{ee} neglecting the contribution of transverse plasmons (i.e., by setting $I = I_l$).

For the densities and temperatures displayed in Figure 2, the *ei* collisions are mainly more efficient than the *ee* ones, although the contribution of the *ee* collisions into the total thermal conductivity is noticeable. One can see that the *ei* collisions are more important for heavier elements (because the Coulomb *ei* scattering cross section is much higher than the *ee* scattering cross section for high-Z elements; see Lampe [13]). The *ee* collisions would be negligible for the iron plasma if the data for this plasma were displayed in Figure 2. The *ee* collisions are more efficient in the helium plasma than in the carbon plasma because the helium ions have lower charges. For a given chemical composition, κ_{ee} gives highest contribution into κ_e at temperatures T a few times lower than T_{pe} (we have $\log_{10} T_{pe}[{\rm K}] \approx 7.86$ and 8.32 at $\rho = 10^5$ and 10^6 g cm^{-3}, respectively). These temperatures separate the high-temperature and low-temperature *ee* collision regimes (e.g., the regimes I and II in the non-relativistic electron gas, see Table I). For $\rho = 10^5$ g cm^{-3}, the electron gas is only slightly relativistic. Accordingly, the contribution of the Landau damping (transverse plasmons) into κ_{ee} is relatively small, and the results of Lampe [13] are sufficiently accurate. For higher $\rho = 10^6$ g cm^{-3}, the contribution of the Landau damping becomes more important which invalidates the previous results of Refs. [14, 15]. In this case the Landau damping strongly reduces κ_{ee} which makes the *ee* collisions much more important for thermal conduction than it was thought before. For still higher ρ the contribution of κ_{ee} into κ_e in a plasma of light elements at $T \sim T_{pe}$ would be even more significant. However, the temperature T_{pe} would
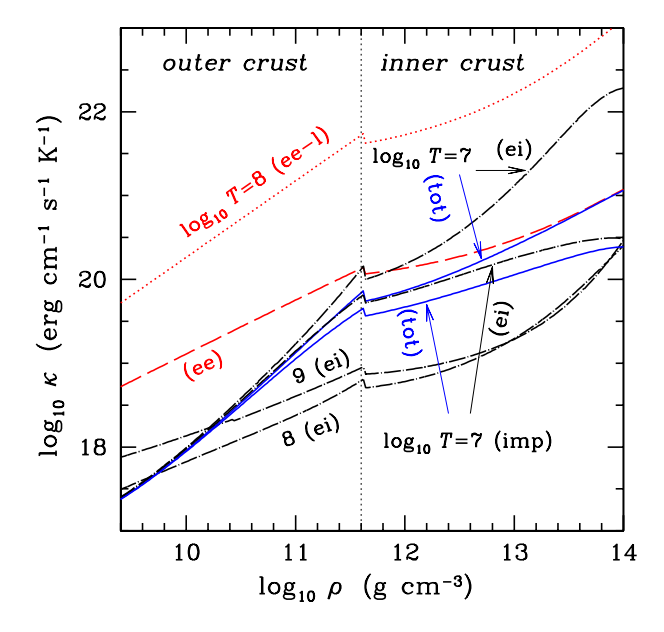
become so high that light elements would start burning in thermonuclear reactions. Therefore, *ee* collisions can noticeably decrease the electron thermal conductivity at densities and temperatures important for nuclear burning of light elements (for instance, in the vicinity of the carbon ignition curve). This should be taken into account in simulations of nuclear evolution of stars (e.g., carbon ignition in white dwarfs [4]).

Figure 3 shows the density dependence of the electron thermal conductivity in the density range from $\sim 2.5 \times 10^9$ g cm^{-3} to 10^{14} g cm^{-3} for the three values of the temperature $T = 10^7$, 10^8, and 10^9 K. We employ the same model of ground-state matter as in Figure 1. The displayed density range is appropriate to a crust of a neutron star. The vertical dotted line is the neutron drip point which separates the crust into the outer and inner parts. The adopted values of T and ρ refer to the regime IV of the *ee* collisions, where the electron gas is ultrarelativistic, $T \ll T_{pe}$, and the Landau damping dominates. The conductivity κ_{ee} (the dashed line) is well approximated by the temperature indepen-

dent conductivity (20) governed by the Landau damping; κ_{ee} slightly deviates from Eq. (20) only at lowest ρ for $T = 10^9$ in Figure 3, where T is still insufficiently lower than T_{pe} (see Figure 1). Retaining the longitudinal contribution into κ_{ee} ($I = I_l$) and setting $T = 10^8$ K, we would get the dotted curve in Fig. 3. It goes much higher than the dashed curve indicating that this longitudinal contribution is really insignificant.

For comparison, the dot-and-dashed lines in Figure 3 give the thermal conductivity κ_{ei} (mostly from Figure 4 of Ref. [6]) for the same values of T, and the solid lines give the total conductivity κ_e. For $T = 10^8$ and 10^9, the effects of possible impurities in dense matter (atomic nuclei with charge numbers Z_{imp} different from charge numbers Z_i of ground-state nuclei) are expected to be small (e.g., Gnedin et al. [6]). At $T = 10^7$ K, the effects of impurities can be substantial. For this T in Figure 3 we present κ_{ei} and κ_e for pure ground-state matter and also for the matter which contains impurities with $|Z_{imp} - Z_i| = 2$ and with the fractional number of impurity nuclei of $n_{imp}/n_i = 0.05$. The impurities increase the ei collision rate and decrease the conductivities κ_{ei} and κ_e.

As seen from Figure 3, κ_{ei} is more important than κ_{ee} at all displayed densities for $T = 10^8$ and 10^9 K. In these cases $\kappa_e \approx \kappa_{ei}$ and we do not show κ_e to simplify the figure. However, κ_{ee} dominates in the pure ground-state matter for $T = 10^7$ K at $\rho \gtrsim 10^{12}$ g cm^{-3} (in the inner crust of a neutron star). This dominance is fully produced by the Landau damping of transverse plasmons in the ee-collisions. For $\rho \gtrsim 10^{13}$ g cm^{-3} in this case we have $\kappa_e \approx \kappa_{ee}$. For an impure cold-catalyzed matter κ_{ei} remains important for all densities at $T = 10^7$ K, but κ_{ee} is comparable to κ_{ei} in the inner neutron star crust. Note that the values of κ_{ei} in Figure 3 take into account, in an approximate manner, the freezing of Umklapp processes in electron-phonon scattering at low temperatures (see, e.g., Ref. [6]). For $T \gtrsim 10^8$ K the freezing is unimportant, but at $T \sim 10^7$ K it enhances κ_{ei}. A more rigorous treatment of this freezing can partly remove this enhancement (A. I. Chugunov, private communication), which can somewhat decrease κ_{ei} and reduce the importance of κ_{ee}.

Therefore, a correct treatment of ee collisions can considerably reduce the electron thermal conductivity in a cold neutron star crust, with $T \sim 10^7$ K. This can increase the time of heat diffusion from the inner crust to the surface [9]. In particular, the effect can be important for the propagation of thermal waves produced by pulsar glitches and for the emergence of these waves on the pulsar surface. The emergence can be, in principle, observed and give valuable information on the nature of pulsar glitches [8].

While calculating κ_{ee} we have taken into account only the electron contribution into the polarization functions Π_l and Π_t in Eq. (6) and neglected the ion contribution. As shown by Lampe [13] this is a good approximation at high temperatures $T \gtrsim Z^2 e^2/(ak_B)$ at which the ions are weakly coupled and constitute a Boltzmann gas. The calculation of the ion polarization functions at lower T (in the regime of strong ion coupling, in an ion liquid or solid) is a complicated problem whose detailed solution is still absent. We have also neglected the effects of strong magnetic fields which can greatly modify electron heat transport in strongly magnetized neutron star envelopes. These effects are numerous (e.g., Yakovlev and Kaminker [26]) and are subdivided into classical (owing to rapid electron Larmor rotation) and quantum ones (owing to the Landau quantization of electron motion in a magnetic field). In principle, a proper treatment of ee collisions in a strong magnetic field can be performed in the same framework of the dynamical plasma screening as used above. However, the problem becomes much more complicated because the electron polarization tensor in a magnetic field is anisotropic (depends on the relative orientations of the wavevector $\boldsymbol{q}$ and the magnetic field) and cannot be generally decomposed into purely longitudinal and transverse parts [21]. The effects of ion polarization and strong magnetic fields are outside the scope of the present paper.

V. CONCLUSIONS

We have reconsidered the electron thermal conductivity κ_{ee} of degenerate electrons produced owing to the ee collisions taking into account the Landau damping due to the exchange of transverse plasmons (following the calculations of kinetic properties of quark plasma by Heiselberg and Pethick [17]). The Landau damping has been neglected in all previous calculations of κ_{ee}. We have analyzed the four regimes of the ee collisions in the degenerate electron gas (Section III, Table I) and obtained analytic expressions for κ_{ee} which accurately approximate the results of numerical calculations of κ_{ee} in wide ranges of the temperature and density of the matter. These results can be applied to study thermal conduction of degenerate electrons in metals, semiconductors, in degenerate cores of evolved stars and white dwarfs, and in envelopes of neutron stars.

Our main conclusions are the following.

(1) The Landau damping strongly modifies κ_{ee} in a relativistic degenerate electron gas, at densities $\rho \gtrsim 10^6$ g cm^{-3}, but it is also quite noticeable at lower ρ (for instance, at $\rho = 10^5$ g cm^{-3}, see Figure 2). The Landau damping increases the ee collision rate and decreases κ_{ee}, increasing the contribution of the ee collisions into the total electron thermal conductivity κ_e.

(2) The most dramatic effect of the Landau damping on κ_{ee} takes place at $\rho \gg 10^6$ g cm^{-3} for temperatures T much below the electron plasma temperature T_{pe} (the regime IV, Table I). In this case κ_{ee} shows a non-Fermi-liquid behavior; it becomes temperature independent and is described by the asymptotic expression (20).

(3) The conductivity κ_{ee} becomes comparable to the electron thermal conductivity κ_{ei} provided by the

electron-ion collisions (and gives thus a noticeable contribution into the total conductivity κ_e) in a warm plasma of light (low-Z) ions at temperatures T a few times lower than T_{pe} (Figure 2). These conditions are typical for degenerate cores of white dwarfs and giant stars where thermonuclear burning of light elements can occur (particularly, in the vicinity of the carbon ignition curve).

(4) The conductivity κ_{ee} dominates over κ_{ei} and determines the total electron thermal conductivity κ_e of the dense pure cold-catalyzed matter at $T \sim 10^7$ K and $\rho \gtrsim 10^{12}$ g cm^{-3} (in the inner crust of a cold neutron star, Figure 3). At these T and ρ the conductivity κ_{ee} is important even for impure cold-catalyzed matter. It can affect the propagation of thermal waves, excited in the inner neutron star crust during pulsar glitches, to the pulsar surface.

The electron conductivity κ_e operates also in neutron star cores, at $\rho \gtrsim 1.5 \times 10^{14}$ g cm^{-3}. This conductivity should also be reconsidered taking into account the Landau damping. Our present results cannot be directly applied to this case because in the cores the electrons collide efficiently at least with degenerate electrons, muons, and protons, and these collisions deserve a special study. We intend to analyze them in a subsequent publication.

[1] J. M. Ziman, *Electrons and Phonons* (Oxford Univ. Press, Oxford, 1960).
[2] E. M. Lifshitz and L. P. Pitaevskiĭ, *Physical Kinetics* (Butterworth-Heinemann, 1981).
[3] P. G. Prada Moroni and O. Straniero, Astrophys. J. **581**, 585 (2002).
[4] I. Baraffe, A. Heger, and S. E. Woosley, Astrophys. J. **615**, 378 (2004).
[5] J. M. Lattimer, K. A. Van Riper, M. Prakash, and M. Prakash, Astrophys. J. **425**, 802 (1994).
[6] O. Y. Gnedin, D. G. Yakovlev, and A. Y. Potekhin, Mon. Not. R. Astron. Soc. **324**, 725 (2001).
[7] D. Page, U. Geppert, and F. Weber, Nucl. Phys. A. (to be published); astro-ph/0508056.
[8] M. B. Larson and B. Link, Mon. Not. R. Astron. Soc. **333**, 613 (2002).
[9] G. Ushomirsky and R. E. Rutledge, Mon. Not. R. Astron. Soc. **325**, 1157 (2001).
[10] T. E. Strohmayer and L. Bildsten, in *Compact Stellar X-Ray Sources*, edited by W. H. G. Lewin and M. van der Klis (Cambridge Univ. Press, Cambridge, in press); astro-ph/0301544.
[11] D. Page and A. Cumming, Astrophys. J. **635**, 157 (2005).
[12] A. Y. Potekhin, D. A. Baiko, P. Haensel, and D. G. Yakovlev, Astron. Astrophys. **346**, 345 (1999).
[13] M. Lampe, Phys. Rev. **170**, 306 (1968).
[14] E. Flowers and N. Itoh, Astrophys. J. **206**, 218 (1976).
[15] V. A. Urpin and D. G. Yakovlev, Sov. Astron. **24**, 126 (1980).
[16] F. X. Timmes, Astrophys. J. **390**, 107 (1992).
[17] H. Heiselberg and C. J. Pethick, Phys. Rev. D **48**, 2916 (1993).
[18] P. Jaikumar, C. Gale, and D. Page, Phys. Rev. D **72**, 123004 (2005).
[19] S. L. Shapiro and S. A. Teukolsky, *Black Holes, White Dwarfs, and Neutron Stars* (New York, Wiley-Interscience, 1983).
[20] V. B. Berestetskiĭ, E. M. Lifshitz, and L. P. Pitaevskii, *Quantum Electrodynamics* (Butterworth-Heinemann, Oxford, 1982).
[21] A. F. Alexandrov, L. S. Bogdankevich, and A. A. Rukhadze, *Principles of Plasma Electrodynamics* (Springer-Verlag, Berlin, Heidelberg, New York, Tokyo, 1984), Springer Series in Electrophysics, Vol. 9.
[22] G. Baym and C. Pethick, *Landau Fermi-Liquid Theory. Concept and Applications* (Wiley Interscience, New York, 1991).
[23] P. Haensel and B. Pichon, Astron. Astrophys. **283**, 313 (1994).
[24] J. W. Negele and D. Vautherin, Nucl. Phys. A **207**, 298 (1973).
[25] A. D. Kaminker, C. J. Pethick, A. Y. Potekhin, V. Thorsson, and D. G. Yakovlev, Astron. Astrophys. **343**, 1009 (1999).
[26] A. D. Kaminker and D. G. Yakovlev, in *Equation of State in Astrophysics*, edited by G. Chabrier and E. Schatzman (Cambridge University Press, Cambridge, 1994), p. 214.